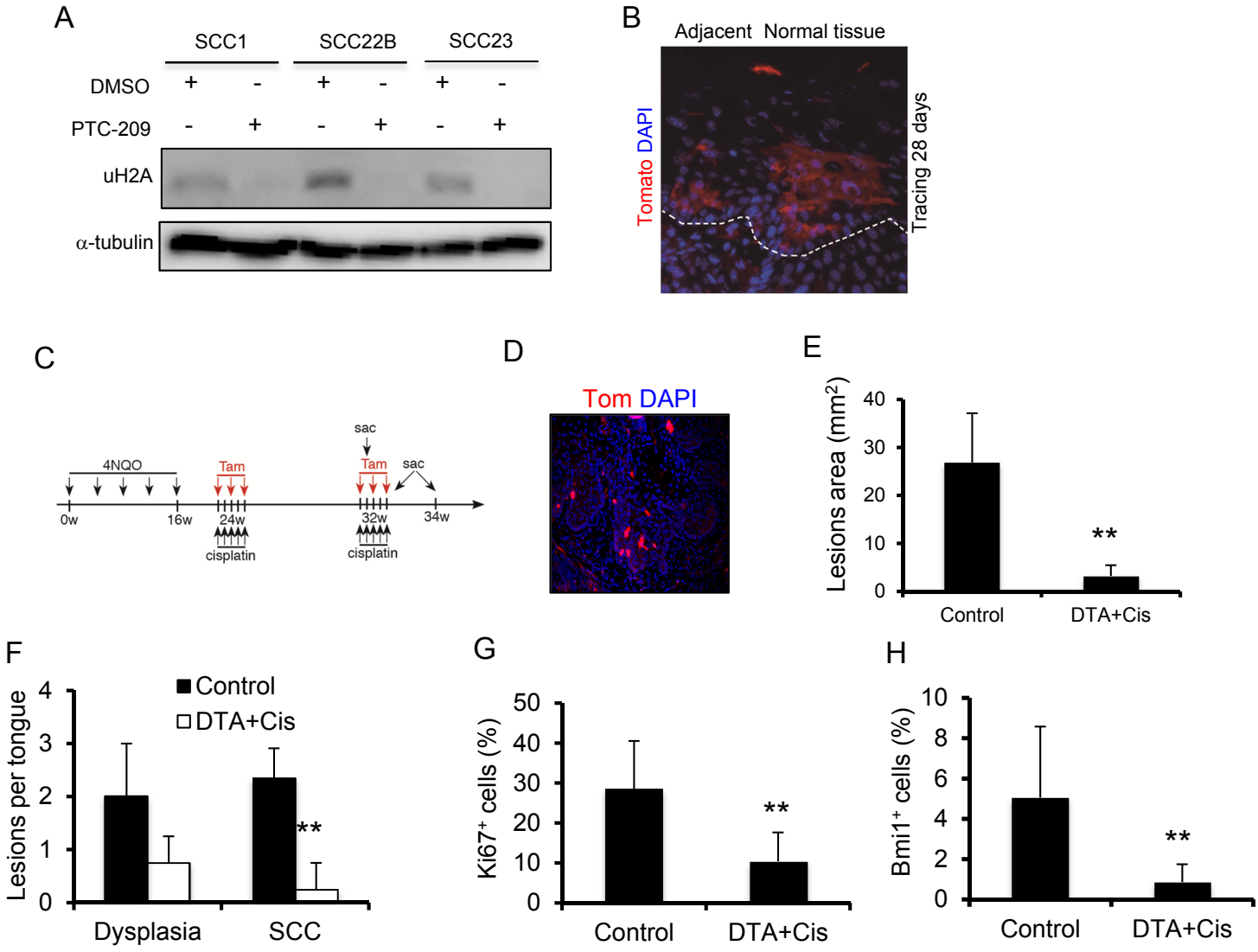

Figure S1, related to Figure 4, The combination of cisplatin and ablating Bmi1⁺ CSCs potently inhibits recurrent HNSCC tumor growth.

(A) PTC-209 suppressed the ubiquitination of histone H2A in HNSCC cells by inhibiting BMI1 activity.

(B) Lineage tracing showed that PTC-209 did not affect adjacent normal epithelial tissues.

(C) Experimental design for examining tumor cells in recurrent HNSCC after ablating Bmi⁺1 CSCs and cisplatin treatment. *Bmi1*^{CreER};*R26*^{DTA} or *Bmi1*^{CreER};*R26*^{tdTomato};*R26*^{DTA} mice after first round of cisplatin and tamoxifen treatment were maintained for 8 additional weeks. Mice with recurrent HNSCC lesion received second round of treatment and tumors were harvested after 1 or 14 days.

(D) Tomato labeling showed Bmi1⁺ CSCs in recurrent HNSCC of mice.

(E) Quantification of recurred lesion areas visible in the tongue 14 days after control (n=3) or cisplatin and ablating Bmi1⁺ CSCs (n=4). Values are mean ± SD. **p < 0.01; Student's t-test.

(F) Quantification of dysplasia and SCC numbers after control (n=3) or cisplatin and ablating Bmi1⁺ CSCs (n=4). Values are mean ± SD. **p < 0.01; Student's t-test.

(G) Percentage of Ki67⁺ cells in recurrent HNSCC of mice 14 days after control or cisplatin and ablating Bmi1⁺ CSCs. Values are mean ± SD. **p < 0.01; Student's t-test.

(H) Percentage of Bmi1⁺ cells in recurrent HNSCC of mice 14 days after control or cisplatin and ablating Bmi1⁺ CSCs. Values are mean ± SD. **p < 0.01; Student's t-test.

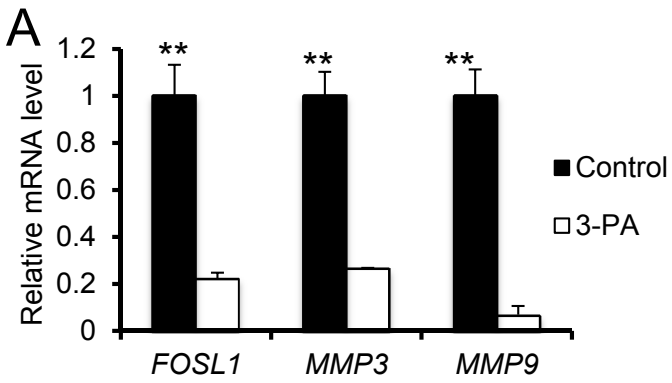

Figure S2, related to Figure 6, 3-PA potently inhibits AP-1 activities in Bmi1^{+} CSCs by Real-time RT-PCR. Data represent mean ± SD from one of three independent experiments. **p < 0.01; Student's t test; n = 3

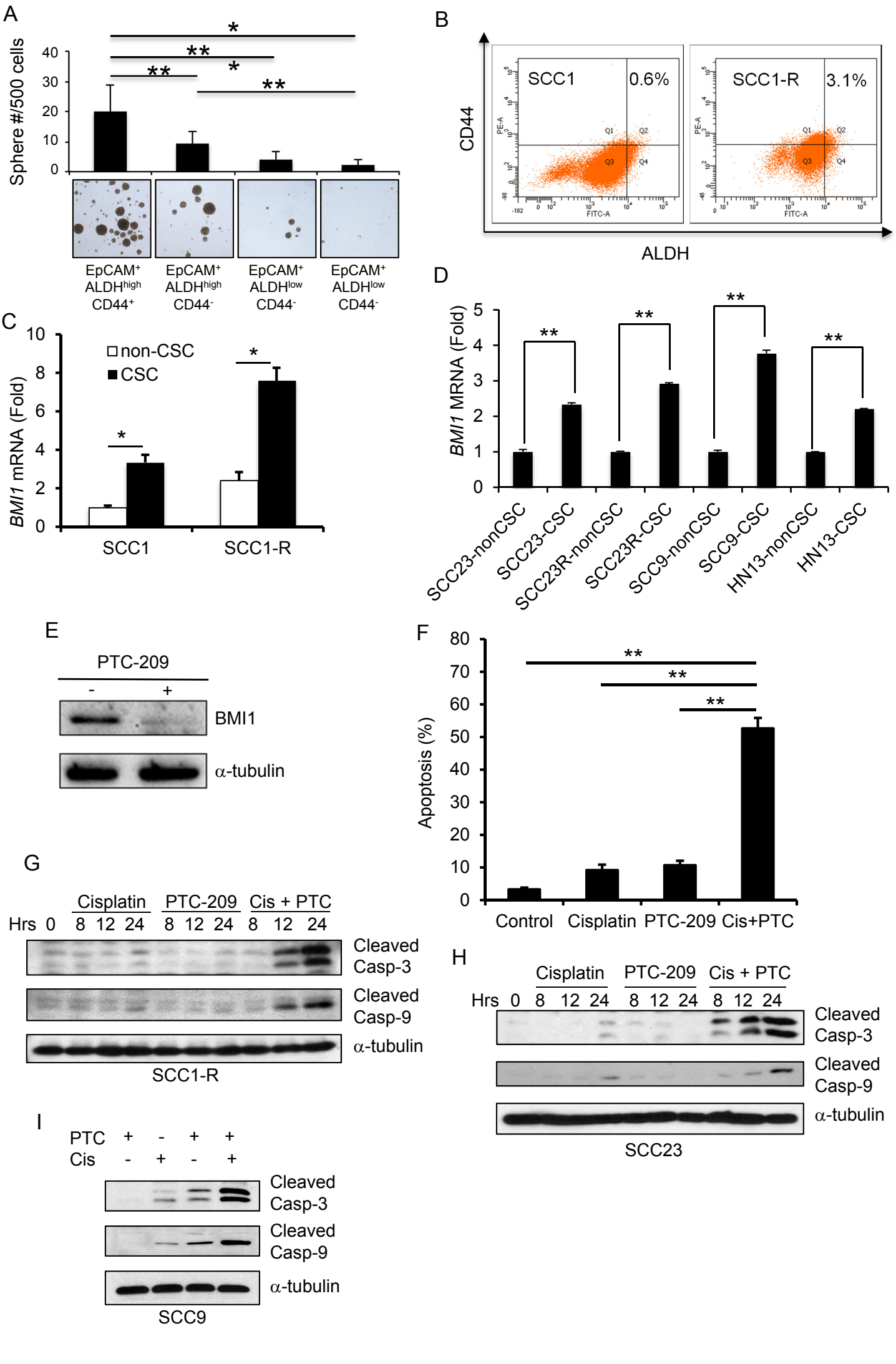
A
Sphere #/500 cells
EpCAM+ ALDHhigh CD44+
EpCAM+ ALDHhigh CD44-
EpCAM+ ALDHlow CD44-
EpCAM+ ALDHlow CD44-
B
CD44
ALDH
SCC1
0.6%
SCC1-R
3.1%
C
BMI1 mRNA (Fold)
non-CSC
CSC
SCC1
SCC1-R
D
BMI1 MRNA (Fold)
SCC23-nonCSC
SCC23-CSC
SCC23R-nonCSC
SCC23R-CSC
SCC9-nonCSC
SCC9-CSC
HN13-nonCSC
HN13-CSC
E
PTC-209
BMI1
α-tubulin
F
Apoptosis (%)
Control
Cisplatin
PTC-209
Cis+PTC
G
Cisplatin
PTC-209
Cis + PTC
Hrs 0 8 12 24 8 12 24 8 12 24
Cleaved Casp-3
Cleaved Casp-9
α-tubulin
SCC1-R
H
Cisplatin
PTC-209
Cis + PTC
Hrs 0 8 12 24 8 12 24 8 12 24
Cleaved Casp-3
Cleaved Casp-9
α-tubulin
SCC23
I
PTC + - + +
Cis - + - +
Cleaved Casp-3
Cleaved Casp-9
α-tubulin
SCC9

Figure S3, related to Figure 7, Inhibition of Bmi1^{+} by PTC-209 renders HNSCC cell lines sensitive to cisplatin.

(A) ALDH^{high}/CD44^{+} cells isolated from primary HNSCC tissues potently formed tumorspheres in vitro compared to ALDH^{high}/CD44^{-}, ALDH^{low}/CD44^{+} and ALDH^{low}/CD44^{-} cells.

(B) FACS sorting showed increasing proportion of ALDH^{high}CD44^{+} cells in SCC1R cells compared to parental SCC1 cells.

(C) qRT-PCR showed that Bmi1 was significantly up-regulated in CSCs in both SCC1 and SCC1R cell lines. Data represent mean ± SD from one of three independent experiments. *$p < 0.05$; Student's t test; n = 3.

(D) Bmi1 expression was elevated in CSCs populations from different HNSCC cell lines. Data represent mean ± SD from one of three independent experiments. **$p < 0.01$; Student's t test; n = 3.

(E) Western blot analysis showed that PTC-209 treatment reduced BMI1 proteins in SCC1R cells.

(F) PTC-209 sensitized SCC1R cells to cisplatin killing. Data represent mean ± SD from one of three independent experiments. **$p < 0.01$; One-way ANOVA; n = 3.

(G) PTC-209 enhanced cisplatin-induced caspase activation in SCC1R cells.

(H) PTC-209 enhanced cisplatin-induced caspase activation in SCC23 cells.

(I) PTC-209 enhanced cisplatin-induced caspase activation in SCC9 cells.

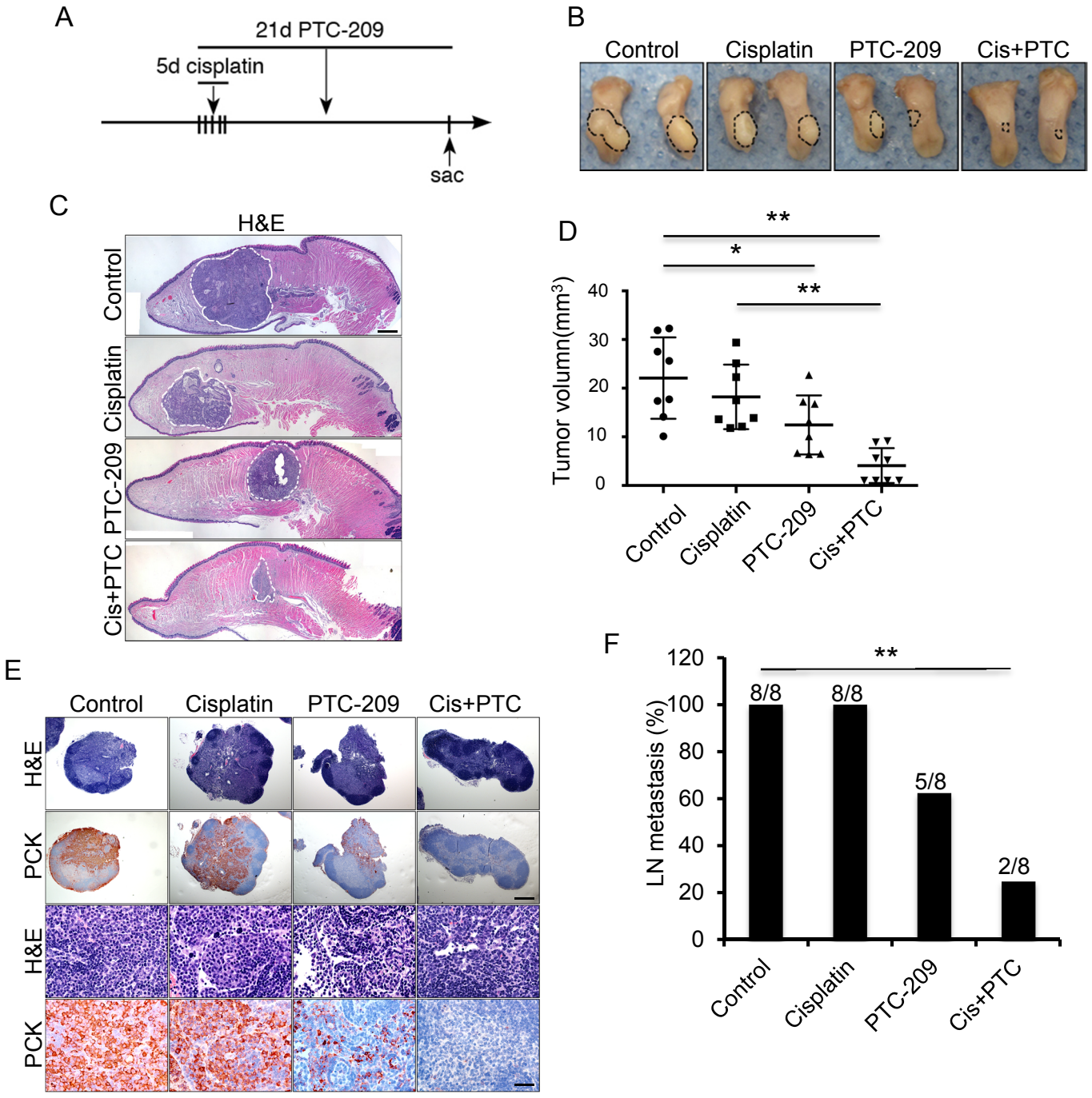

Figure S4, related to Figure 7, Inhibition of BMI1 by PTC-209 impairs tumorigenic and chemoresistant properties of ALDH^{high}CD44^{+} CSC-like cells from a cisplatin-resistant human HNSCC cell line.

(A) Experimental design for SCC1R tumor treatment *in vivo*.

(B) Representative image of HNSCC tumors from ALDH^{high}CD44^{+} CSCs after treatment. Cis+PTC, cisplatin plus PTC-209.

(C) Histologic staining of human HNSCC tumors in nude mice after treatment. Scale bar, 250 μm. Cis+PTC, cisplatin plus PTC-209.

(D) Quantification of human HNSCC tumor growth in nude mice after treatment. Values are mean ± SD. *p < 0.05; one-way ANOVA; n = 8.

(E) Representative staining of metastatic tumor cells in cervical lymph nodes of nude mice after treatment using anti-pan-cytokeratin (PCK). Scale bar upper, 250 μm; Scale bar lower, 50 μm.

(F) The percentage of mice having lymph node metastasis in nude mice after treatment. *p<0.05; Fisher exact test; n =8. Cis+PTC, cisplatin plus PTC-209.

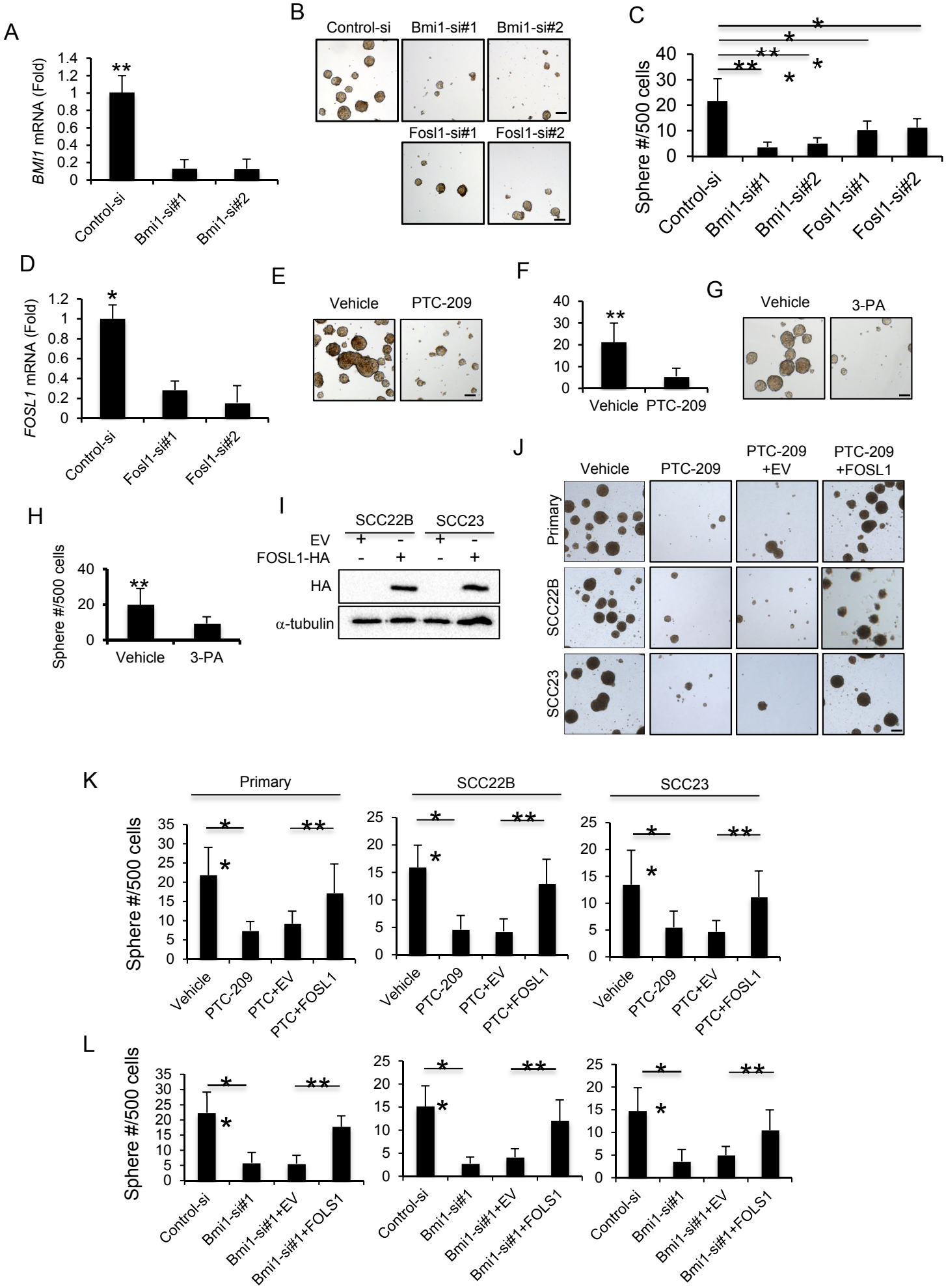
A
BMI1 mRNA (Fold)
Control-si
Bmi1-si#1
Bmi1-si#2
B
Control-si
Bmi1-si#1
Bmi1-si#2
Fosl1-si#1
Fosl1-si#2
C
Sphere #/500 cells
Control-si
Bmi1-si#1
Bmi1-si#2
Fosl1-si#1
Fosl1-si#2
D
FOSL1 mRNA (Fold)
Control-si
Fosl1-si#1
Fosl1-si#2
E
Vehicle
PTC-209
F
Vehicle
PTC-209
G
Vehicle
3-PA
H
Sphere #/500 cells
Vehicle
3-PA
I
SCC22B
SCC23
EV
FOSL1-HA
HA
α-tubulin
J
Vehicle
PTC-209
PTC-209 +EV
PTC-209 +FOSL1
Primary
SCC22B
SCC23
K
Primary
SCC22B
SCC23
Sphere #/500 cells
Vehicle
PTC-209
PTC+EV
PTC+FOSL1
L
Sphere #/500 cells
Control-si
Bmi1-si#1
Bmi1-si#1+EV
Bmi1-si#1+FOLS1

Figure S5, related to Figure 7, Targeting BMI1 or AP-1 impairs tumor sphere formation of human CSCs in vitro.

(A) Real-time RT-PCR showed that *BMI1* mRNA from human CSCs was knocked down by two different *BMI1* siRNAs. Data represent mean ± SD from one of three independent experiments. **p < 0.01; Student's t test; n = 3.

(B) Representative images of tumor sphere formation by *BMI1* and *FOSL1* knockdown human CSCs.

(C) Quantification of tumor sphere formation of human CSCs after knockdown of *BMI1* or *FOSL1*. Values are mean ± SD from one of three independent experiments. *p < 0.05; **p < 0.01; one-way ANOVA; n = 12.

(D) Real-time RT-PCR confirmed that *FOSL1* mRNA from human CSCs was knocked down by two different *FOSL1* siRNAs. Data represent mean ± SD from one of three independent experiments. **p < 0.01; Student's t test; n = 3.

(E and F) PTC-209 treatment inhibited tumorsphere formation of human CSCs. Data represent mean ± SD from one of three independent experiments. **p < 0.01; Student's t test; n = 3.

(G and H) 3-PA treatment inhibited tumor sphere formation of human CSCs. Data represent mean ± SD from one of three independent experiments. **p < 0.01; Student's t test; n = 3.

(I) The ectopic expression of HA-FOSL1 in HNSCC cells was determined by Western blot.

(J and K) The ectopic expression of FOSL1 rescued tumorsphere formation inhibited by PTC-209. Data represent mean ± SD from one of three independent experiments. *p < 0.05, **p < 0.01; Student's t test; n = 3.

(L) The ectopic expression of FOSL1 rescued tumorsphere formation inhibited by Bmi1 knockdown. Data represent mean ± SD from one of three independent experiments. **p < 0.01; Student's t test; n = 3.

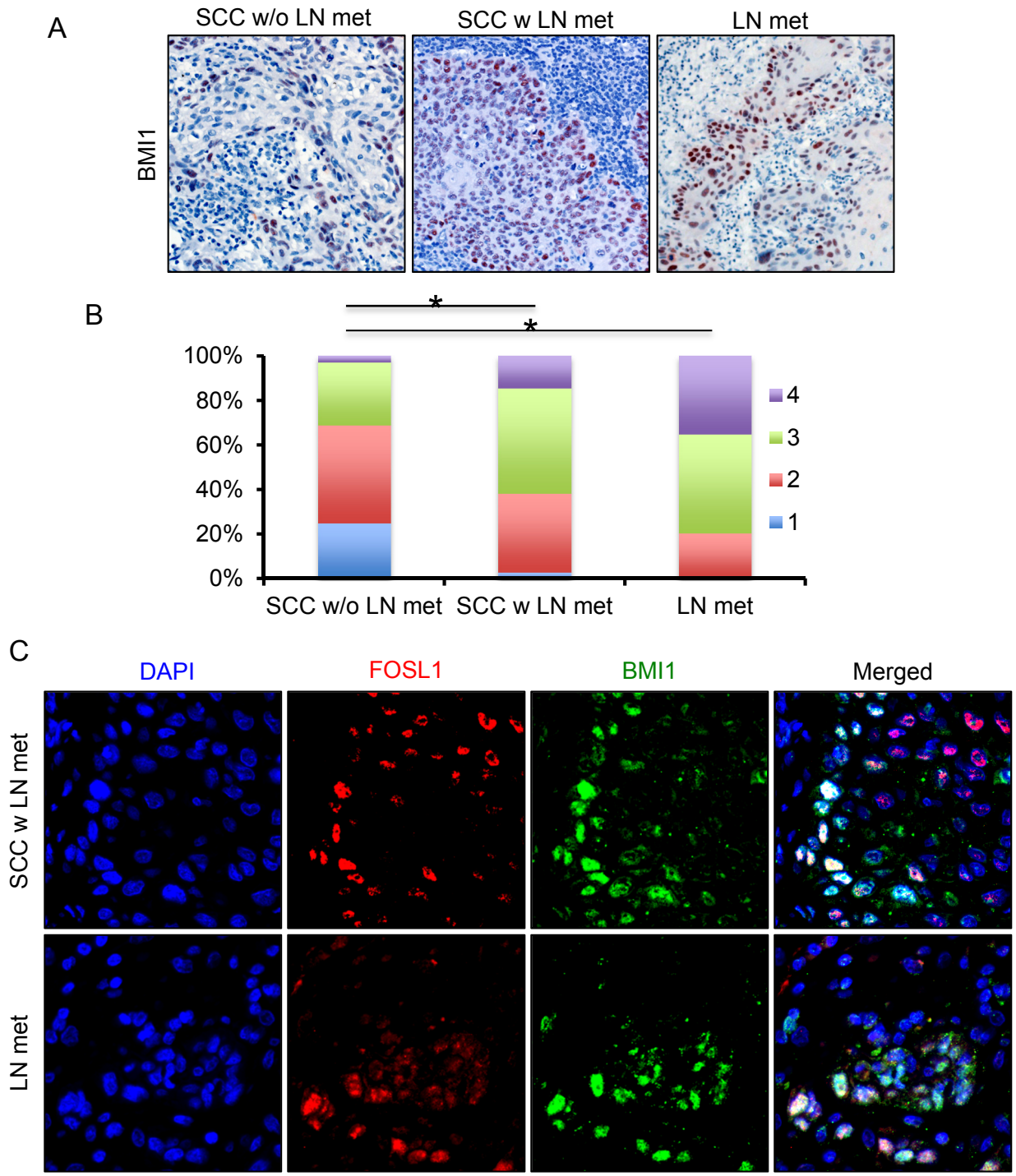

Figure S6, related to Figure 7, BMI1 is highly abundant in human SCC lymph node metastasis and co-expressed with FOLS1.

(A) Immunostaining of BMI1 expression in human HNSCC specimens without LN metastasis (SCC w/o LN met), HNSCC with lymph node metastases (SCC w LN met) and lymph node metastases (LN met). Images are representative of 31 (SCC w/o LN met), 33 (SCC w LN met), and 33 (LN) samples.

(B) Quantification of BMI1 abundance in SCC w/o LN met, SCC w LN met and lymph node metastases (LN met). BMI1 staining intensity was scored as: 1 = weak; 2 = moderate; 3 = strong staining and 4 = very strong.

(C) Co-immunostaining for FOSL1 (red) and BMI1 (green) in HNSCC with lymph node metastases (SCC w LN met) and lymph node metastases (LN met).

Table S1, related to Figure 6. Differential expressed genes between Tomato^{+} and Tomato^{-} tumor cells.

Table S2, related to Figure 7, BMI1 is positively correlated with the levels of FOSL1 in HNSCC by Pearson correlation analysis (r = 0.796, p < 0.01).

Table S2, related to Figure 7, The abundance of BMI1 correlates with the abundance of FOSL1 in human HNSCC

		FOSL1 expression			
		1	2	3	4
BMI1 expression	1	0	9	0	0
	2	0	7	26	0
	3	0	0	27	13
	4	0	0	0	15

The staining intensity was scored as: 1, weaker staining; 2, modest staining; 3, strong staining; and 4 very strong staining. r=0.7960; p<0.01